Genetically encoded protein oscillators for FM streaming of single-cell data

Rohith Rajasekaran[1,2], Thomas M. Galateo[1], Zhejing Xu[1,2], Dennis T. Bolshakov[1,3], Elliott W. Z. Weix[1], Scott M. Coyle[1,*]

Affiliations:
[1]Department of Biochemistry
[2]Integrated Program in Biochemistry Graduate Program
[3]Cellular and Molecular Biology Graduate Program

University of Wisconsin-Madison, Madison, Wisconsin 53706, USA.
*Correspondence to: smcoyle@wisc.edu

Abstract.

Radios and cellphones use frequency modulation (FM) of an oscillating carrier signal to reliably transmit multiplexed data while rejecting noise. Here, we establish a biochemical analogue of this paradigm using genetically encoded protein oscillators (GEOs) as carrier signals in circuits that enable continuous, real-time FM streaming of single-cell data. GEOs are constructed from evolutionarily diverse MinDE-family ATPase and activator modules that generate fast synthetic protein oscillations when co-expressed in human cells. These oscillations serve as a single-cell carrier signal, with frequency and amplitude controlled by GEO component levels and activity. We systematically characterize 169 ATPase/activator GEO pairs and engineer composite GEOs with multiple competing activators to develop a comprehensive platform for waveform programming. Using these principles, we design circuits that modulate GEO frequency in response to cellular activity and decode their responses using a calibrated machine-learning model to demonstrate sensitive, real-time FM streaming of transcription and proteasomal degradation dynamics in single cells. GEOs establish a dynamically controllable biochemical carrier signal, unlocking noise-resistant FM data-encoding paradigms that open new avenues for dynamic single-cell analysis.

Introduction.

Cells dynamically regulate gene expression, protein localization, and signaling state across different timescales to perform essential biological functions[1–4]. While genomic, transcriptomic and proteomic methods can provide snapshots of single cell states[5–8], the ability to follow the trajectories of individual cells in real time is critical to understanding how dynamic cellular and organismal behaviors are encoded and function[1,9,10]. These single-cell dynamics are often tracked microscopically using fluorescent reporters whose intensity or localization provides a proxy for the data of interest[10–16]. While powerful, these tools present challenges for extended tracking of single-cell dynamics and data aggregation, as arbitrary signal intensity varies across instruments and is sensitive to photobleaching and noise[17]. Moreover, the signals generated by traditional fluorescence-based tools lack metadata for identifying the underlying cellular source of the signal, making separation of overlapping signals in dense cellular environments difficult.

Electrical engineers overcome similar challenges in telecommunications by coupling data of interest to changes in the frequency of an easily measured carrier oscillation[18–20]. Because data is encoded in the temporal structure of the oscillation, frequency modulation (FM) has the advantage that measurements are in non-arbitrary units (ΔHz) and robust against noise and fluctuating intensity, making them consistent across different contexts and instruments. In addition, by assigning different carrier frequencies to different senders, multiple independent streams of FM data can be transmitted in the same medium and reliably unmixed using a range of powerful signal processing techniques. Extending FM data-encoding capabilities to biological measurement would provide a powerful paradigm for measuring single-cell dynamics and defining their biological consequences. However, such approaches would require a biochemical analogue to the electromagnetic waves that serve as carrier signals in radios and cellphones.

Recently, we have shown that synthetic protein waves can be robustly generated in human cells by expression of the orthogonal *E. coli* divisome positioning system MinDE[21]. In this system, an ATPase (MinD) and its ATPase-activator (MinE) self-organize ATP-driven propagation of protein waves across cell membranes that coherently fill the cell interior (Fig. 1A)[22–25]. These waves produce a persistent single-cell oscillation with a unique frequency and amplitude specified by the expression levels of the MinDE components (Fig. 1A). Critically, these oscillations are fast (seconds to minutes), amenable to synthetic control and protein engineering, and can be analyzed using signal processing tools such as Fast Fourier Transform (FFT) and Continuous Wavelet Transform (CWT)[21]. While this opens the possibility of using these waves as single-cell carrier

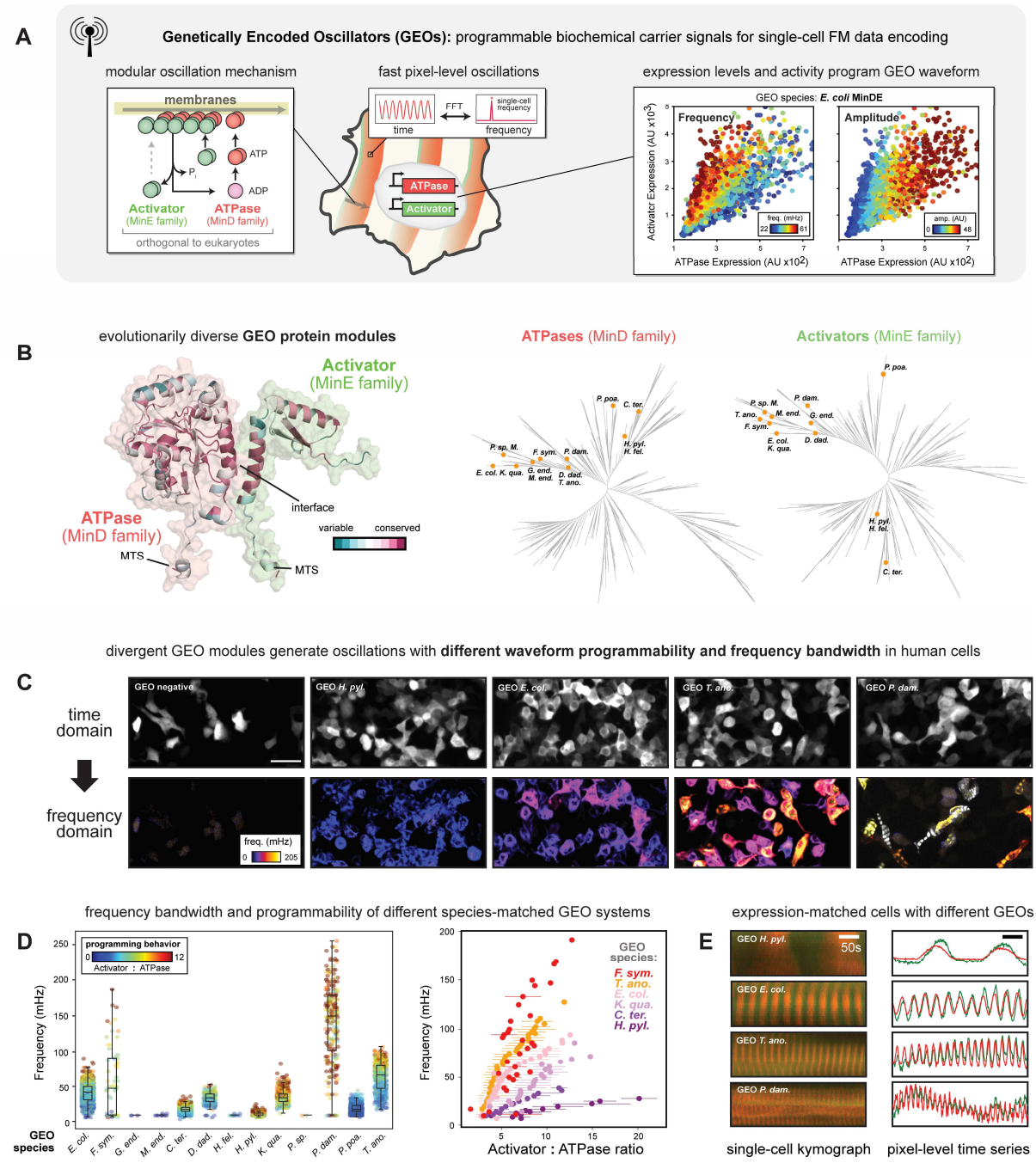

Figure 1. Evolutionarily diverged GEOs expand the functional space available for synthetic spatiotemporal cell circuit design. (A) The MinD ATPase and its activator MinE form a Genetically Encoded Oscillator (GEO) pair that generates oscillatory waveforms when transplanted into human cells. These protein oscillations provide a synthetic biology platform for engineering complex spatiotemporal circuits that barcode and broadcast host cell signaling activity. Aggregating single-cell circuit behavior across thousands of 293T cells reveals how GEO circuit frequency and amplitude are programmed at the genetic and protein level by ATPase and Activator expression. Phase portraits for *E. coli* GEO frequency and amplitude are shown. Functional space and detailed quantitative trends for programming dynamic behavior are fixed by specific GEO protein sequence identity. (B) ConSurf analysis of GEO sequence diversity using phylogenetic trees and multiple sequence alignments is mapped onto AlphaFold2 structure prediction of *E. coli* GEO dimer. 4585 unique MinD ATPase sequences and 4331 unique MinE Activator sequences were aligned using ClustalW. Phylogenetic trees were built using the JTT matrix for maximum likelihood, and rapid bootstraps (100 replicates) with gamma substitution rates were used for tree construction. 13 selected species-matched GEO pairs are annotated. (C) Representative widefield fluorescence images and false-colored image power spectrum taken from 293T cells transiently transfected with different species-matched GEO pairs (GEO negative pair: mCherry and GFP expression). (scale bar: 50μM) (D) [Activator] to [ATPase] expression ratio is the major determinant of GEO circuit frequency and can be compared across species

signals, the frequency bandwidth and dynamic programmability of the *E. coli* MinDE system in human cells are fundamentally limited and constrained by the biochemistry of the components.

Here we leverage evolutionary diverse ATPase/activator modules within the MinDE family to develop a modular platform for designing and manipulating genetically encoded oscillators (GEOs) to develop circuits that enable continuous FM streaming of single-cell data in human cells. GEO modules can be synthetically recombined or layered into composites to program and dynamically modulate single-cell waveforms. We characterize hundreds of GEO pairs and model their behaviors to develop a comprehensive framework for predictable waveform encoding and manipulation. Engineered GEO-FM circuits can continuously modulate GEO frequency in response to changing cellular activities and the resulting data streams can be decoded using a machine-learning model. We demonstrate GEO-FM circuits that provide multiplexed sensitive readouts of transcriptional activity and proteasomal degradation that are defined in non-arbitrary, transferable units (ΔmHz) and independent of signal intensity. By establishing a platform for dynamic control of a biochemical carrier signal, GEOs unlock sophisticated, noise-resistant FM data-encoding paradigms, opening new avenues for dynamic multiplexed single-cell analysis.

Results.

Evolution provides diverse MinDE ATPase/activators modules for designing genetically encoded oscillators (GEOs).

The *E. coli* ATPase MinD and its activator MinE generate fast synthetic protein waves across membranes when expressed in human cells, providing a compact and orthogonal genetically encoded oscillator (GEO) that could serve as a carrier for FM transmission of biological data[21]. The rules to program and manipulate the frequency and amplitude of these oscillations are defined by the expression levels and biochemistry of the GEO components[21–23]. These biochemical programming rules can be experimentally determined by constructing a phase portrait from imaging thousands of cells, providing a visual landscape of how ATPase and activator levels map to frequency and amplitude (Fig. 1A). The *E. coli* GEO phase portraits reveal how frequency scales as the [Activator] to [ATPase] ratio, with an accessible (5^{th}-95^{th} percentile range) bandwidth spanning 25-58 mHz (Fig. 1A).

To generalize these oscillation systems and expand GEO programmability, we took an evolution-guided approach. We hypothesized that divergent MinDE-family ATPase/activator pairs across different bacterial species would possess altered reaction rates, stability, or membrane preferences that would alter their programming rules[26]. Phylogenetic analysis of thousands of species-matched MinDE pairs revealed extensive diversification of the ATPase and activator modules (Fig. 1B, Fig. S1). Mapping sequence conservation onto a structural model of the ATPase/activator complex suggested general preservation of the overall structure and binding interface but extensive divergence within the individual proteins, especially in their membrane targeting sequences (Fig. 1B, Fig. S1). Thus, we hypothesized that these ATPases and activators could likely act as separable modules for constructing GEOs with different quantitative behaviors and altered programmability.

To explore this, we selected 12 species-matched ATPase/activator pairs with varying levels of sequence similarity to *E. coli* MinDE for phase portrait analysis in 293T cells (Fig. 1B, Fig. S2-3, Movie S1). Of the 12 new GEO pairs tested, 9 robustly supported synthetic wave

---

variants. The frequency-scaling behavior for GEO species-matched pairs are shown. A swarm plot showing single-cell frequency quantification across a population of 293T cells expressing the respective GEO species-matched pair. Individual cells are colored by [Activator] to [ATPase] expression ratio. A variance plot showing variance (mean value ± standard deviation) in [Activator] to [ATPase] expression ratio for cells with the same oscillatory frequency. (E) Representative kymographs and pixel-level time series of GEO expression-level matched cells for different species-matched GEO pairs.

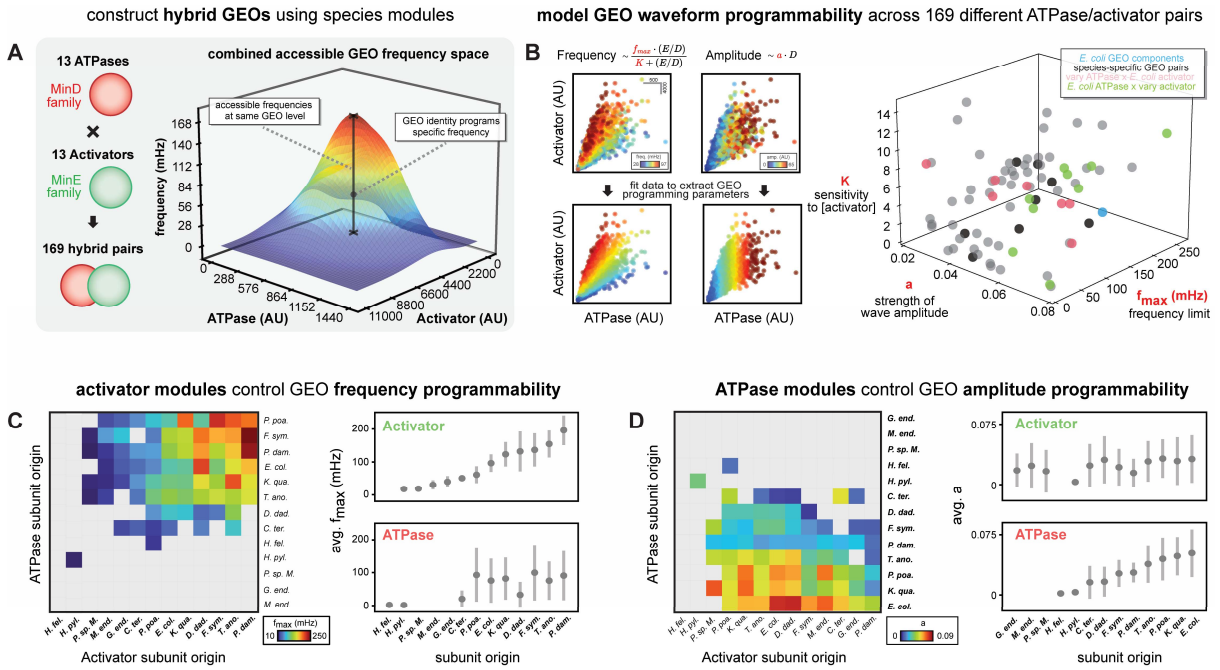

Figure 2. Synthetic recombination of diverged GEO pairs identifies cross-compatible circuit components for quantitative control of dynamic behavior. (A) The ATPase and activator of GEO pairs act as modules for engineering emergent oscillatory dynamics. 169 pairwise combinations of the 13 species-matched ATPase and activator pairs from Fig. 1 were tested. Individual frequency phase portraits associated with each pairwise combination was aggregated to generate a global accessible design space. A 3D surface visualizing the range of accessible frequencies at any GEO expression level using any GEO pairwise combination is shown. (B) GEO waveform frequency and amplitude can be modeled using simple mathematical relationships to extract intuitive programming parameters. A 3D scatterplot of f_{max}, K, and a for 76 functional GEO systems is shown. (C) Hierarchically clustered heatmap depicting f_{max} for 169 pairwise GEO combinations. Average f_{max} calculated for Activator identity and ATPase identity are shown. Subunit origin axis was sorted by ascending average f_{max} of Activator identity. (D) Hierarchically clustered heatmap depicting a for 169 pairwise GEO combinations. Average a calculated for Activator identity and ATPase identity are shown. Subunit origin axis was sorted by ascending average a of ATPase identity.

formation. Strikingly, many of these new GEOs exhibited altered programmability including shifts in the expression levels that supported oscillation and the range of frequencies that could be achieved (Fig. 1C-D, Fig. S3). For example, over the same range of [Activator] to [ATPase] ratios, the *F. symbiotica* GEO had wide accessible bandwidth (11-169 mHz) compared to *E. coli* (25-58 mHz), while *H. pylori* GEO bandwidth was narrow (8-16 mHz). Expression-matched cells harboring different GEO pairs can thus encode oscillations with different frequencies (Fig. 1E).

The level of conservation at the ATPase/activator interaction interface suggested that additional functional GEOs with hybrid behaviors could likely be created by combining ATPase and activator modules from different species. We tested 169 pairwise combinations of the 13 ATPase and activator species in 293Ts and imaged thousands of cells for each hybrid to recover its associated phase portrait. This identified 76 hybrid GEOs that robustly oscillated in the context of 293T cells. Aggregating phase portrait data across all functioning GEO pairs allows construction of a global design manual for programming GEO waveform, with an accessible bandwidth spanning 8-169 mHz at modest expression levels (Fig. 2A). In addition, frequencies as high as 205 mHz could be realized using specific GEO components at defined expression levels (Fig. 1D). Thus, the overall GEO design space can be computationally queried to identify modules that program a target waveform at a given expression level.

This specific GEO design space was constructed using a model 293T cell line. To test the generality of the GEO platform and the transferability of its associated programming rules, we analyzed the behavior of the same panel of 169 GEOs in a completely different budding yeast chassis. In this setting, we observed similar qualitative and quantitative trends to the 293T data

(Fig. S4), suggesting the portfolio of GEO modules in our platform has broad utility for waveform programming across different cell lines and diverse eukaryotes.

To quantitatively characterize and compare GEO behavior across individual hybrids, we developed a phenomenological model to fit the phase portrait for each GEO (Fig. 2B, detailed in Fig. S5). Oscillation *frequency* was treated as a hyperbolic response to the [Activator] to [ATPase] ratio, with f_{max} describing the maximum frequency achievable by a given GEO and K describing the sensitivity of GEO frequency to changes in [Activator]. We modeled oscillation *amplitude* as a linear response to [MinD] with slope parameter a. An associated wave energy can be used to restrict fit predictions only to the regions of expression space where oscillations were experimentally observed to occur (Fig. S6). Using this approach, we reduced the description of each GEO's programming rules and phase portrait down to three intuitive parameters.

A scatterplot of f_{max}, K, and a for the 76 functional GEO systems revealed a wide range of parameters accessible to GEOs for waveform design (Fig. 2B). While species-matched ATPase/activator pairs expanded frequency programmability, inter-species hybrids accessed a significantly wider range and breadth of parameter space. Notably, only interspecies hybrids exhibited larger K values, allowing oscillations to be generated or tuned across a larger range of expression levels. This feature is likely a consequence of imperfections at the binding interface between ATPase and activators that have not co-evolved.

The hybrid screen also revealed how the identity of ATPase and activator modules independently contributed to the GEO waveform. Activator identity was the primary controller of a GEO's frequency bandwidth f_{max} (Fig. 2C). For example, GEOs constructed using the *P. damselae* activator consistently oscillated faster than GEOs constructed with the *E. coli* activator. Sorting activator modules by their average f_{max} across all hybrids provides a hierarchy of activator strengths for predictable design of faster or slower GEOs. In contrast, ATPase identity was the primary controller of a GEO's amplitude parameter (Fig. 2D).

Collectively, our ability to build many functional GEOs from a small set of GEO modules demonstrates the ease with which the frequency-amplitude relationships of these biochemical oscillations can be systematically programmed. These ATPase and activator modules provide a starting point for engineering GEOs with more complex circuit architectures for cell-based data-encoding applications.

Engineered multi-component GEOs enable compositional control of oscillation frequency.

The GEO waveform design space in Fig. 2A is based on single ATPase / single activator pairs. Because our hybrid screen found that different activator modules can cross-react with the same ATPase, we hypothesized that multi-component GEOs would be functional (Fig. 3A). However, it is not obvious whether the biochemical mechanism underlying GEO wave propagation would support multiple competing components or how the resulting oscillations would behave.

To gain intuition, we extended a stochastic model of GEO wave propagation in mammalian cells[21,27,28] to include two chemically distinct activator modules: one that produces slow oscillations (Activator j); and one that produces fast oscillations (Activator k) (Fig. 3B). For simplicity, the only difference between the two activators in this model is in their rate constant for stimulating ATPase activity. Despite no explicit interaction between the two activators, a GEO simulation containing 50% Activator j and 50% Activator k produced a single composite waveform in which the two activators oscillated in phase. This coherence appears to arise through indirect coupling of activators via their shared ATPase node, as simulations using fully decoupled GEOs produced two separate frequencies (Fig. S7). To understand how the relative amount of Activator j and Activator k control the waveform, we performed simulations that titrated the percentage of Activator k in the system from 0 to 100% at steps of 1% (Fig. 3B). We found that the wave frequency was smoothly titrated by the relative composition of the two activators. Thus, for this

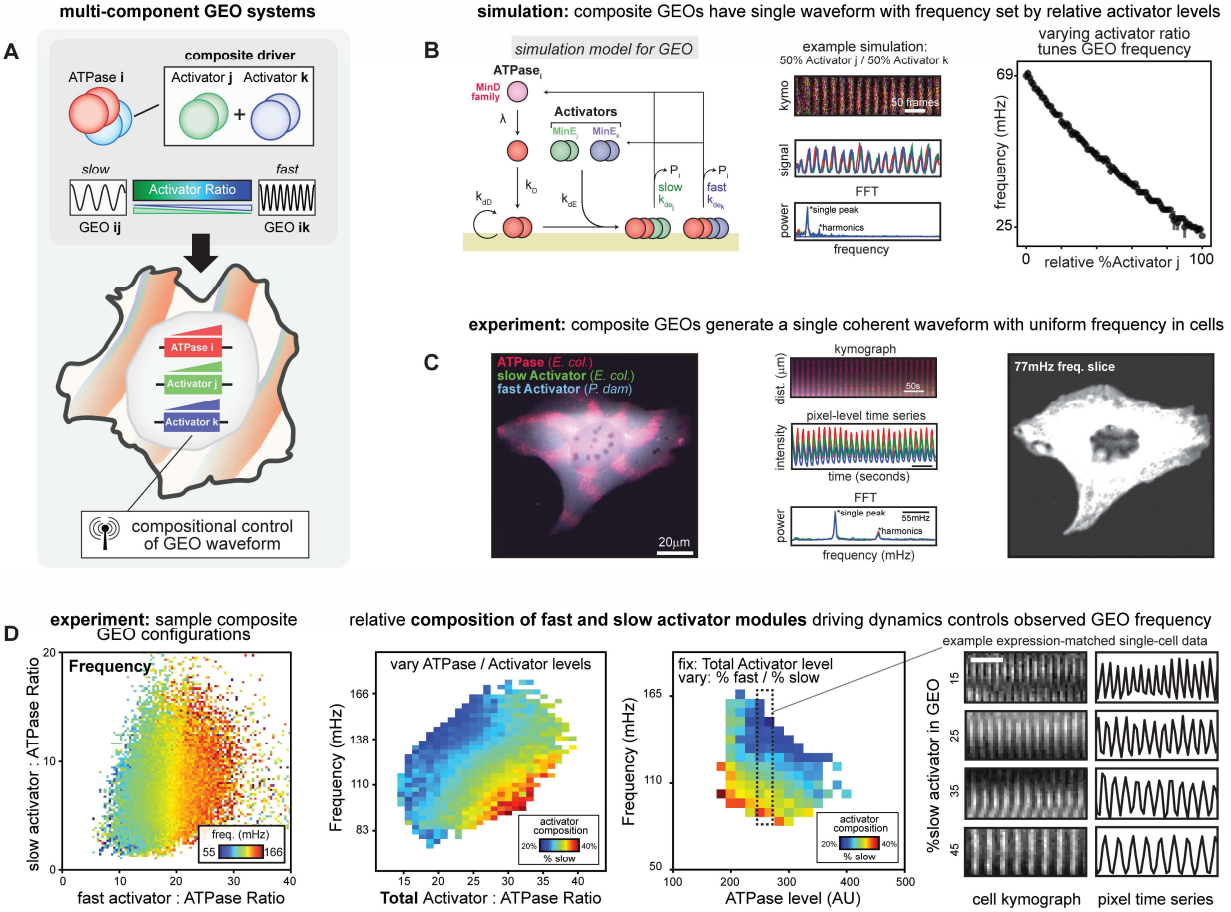

Figure 3. Multi-component GEO patterning systems produce a single waveform quantitatively controlled by relative protein composition. (A) Schematic of a multi-component GEO system built using a single ATPase and a composite driver composed of a mixture of two competing activators. (B) Diagram of the "skeleton model" of the multi-component GEO system, depicting the biochemical species and the reactions that occur. The labels for the molecular species and rate constants associated with the formal description of the simulation equations are indicated. A representative kymograph, pixel-level time series, and the associated FFT power spectrum for an example simulation of 50% Activator j and 50% Activator k is shown. A set of simulations with varying % Activator j was performed. Peak frequency for each respective % Activator j and associated standard deviation is shown (10 replicates). (C) Representative fluorescence image of a U-2 OS cell transduced with a multi-component GEO system composed of an ATPase (*E. coli*), a slow (*E. coli*) activator, and a fast (*P. damselae*) activator. A representative kymograph, pixel-level time series, and the associated FFT power spectrum for this cell is shown. The image power spectra for this cell at the 77 mHz frequency slice is shown. (D) Aggregating single-cell multi-component GEO circuit behavior across thousands of U-2 OS cells reveals how frequency is programmed by protein expression levels. A multi-dimensional phase portrait showing the observed relationship between relative protein expression levels and circuit frequency is shown. The [Total Activator] to [ATPase] expression ratio is a major determinant of GEO frequency. The frequency-scaling behavior for multi-component GEOs with different activator compositions is shown. The frequency dynamics for fixed [Total Activator] level and varying [ATPase] level are shown. Representative kymographs and pixel-level time series for [Activator] and [ATPase] expression-level matched cells with different compositions of Total Activator are shown. (scale bar: 50 seconds)

multi-component GEO, the two activator species can be treated as a composite driver of oscillation frequency whose overall activity is controlled by relative levels of each activator.

Encouraged by these modeling results, we experimentally implemented this multi-component GEO design in human cells (Fig. 3C, Movie S2). From our panel of GEO modules and their cross-reactivity profiles (Fig. 2C), we selected slow (*E. coli)* and fast (*P. damselae*) activators to pair with a single ATPase (*E. coli)*. Consistent with the modeling results, expression of this multi-component GEO in human cells produced a single waveform at one frequency in which the two activator modules co-oscillated in phase (Fig. 3C). By sampling a wide range of expression levels across all three components, we obtained a multi-dimensional phase portrait that

comprehensively describes how GEO composition programs waveform (Fig. 3D, Fig. S8). As in our models, the relative composition of the composite driver controlled the observed frequency of the oscillation (Fig. 3D). This means that the GEO frequency for a cell with identical ATPase and total activator levels can be manipulated by varying the relative composition of the composite driver (Fig. 3D), providing a potential strategy for building frequency-modulation circuits.

GEO-FM circuits enable frequency-modulated streaming of dynamic single-cell data.

The ability to tune the frequency of a multi-component GEO using compositional control suggests a simple and generalizable strategy for building GEO-FM circuits that broadcast frequency-modulated single-cell data streams for dynamic cellular states (Fig. 4A). In this GEO-FM circuit design, constitutive expression of a "slow activator" (*carrier*) will generate a constitutive carrier oscillation inside the cell. Data can be encoded in frequency modulation of this oscillation by coupling the availability of a second "fast activator" (*encoder*) to an endogenous cellular activity of interest. By calibrating the frequency response of GEO-FM circuits, the underlying data of interest can be decoded from the modulated signal. These FM data streams would thus provide barcoded measurements of cellular state in non-arbitrary units (ΔmHz) that are transferable across instruments and insensitive to photobleaching and intensity fluctuations[18,19,29].

To gain intuition and facilitate GEO-FM circuit design, we used our stochastic model of multi-component GEO wave propagation to simulate different GEO-FM data encoding and decoding schemes (Fig. 4B, detailed in Fig. S7). In these simulations, a baseline signal is established using a fixed amount of carrier activator. Then, data in the form of a ramp input of an encoder activator is introduced into the system to modulate the waveform. The resulting change in GEO frequency of the simulated waveform was estimated at every timepoint using Continuous Wavelet Transform (CWT), a time-frequency signal processing method[30,31]. For a fixed input ramp of data to encode, we found that faster encoders led to larger changes in the FM response of the circuit (Fig. 4B). By simulating different ramp inputs of data with a high-sensitivity encoder, different levels and rates of activation could be distinguished in the FM response of the circuit (Fig. 4B). Together, these simulations suggest compositionally controlled GEO-FM circuits could provide a sensitive and versatile system for encoding and decoding dynamic single-cell data streams.

To experimentally deploy GEO-FM circuits for multiplexed single-cell data streaming in mixed populations, the frequency response of a cell's specific carrier signal to changes in encoder level must be calibrated to allow decoding of the biological data of interest. This can be readily achieved by imaging a broad range of ATPase, carrier activator, and encoder activator expression levels and measuring the associated oscillation frequency. From a single imaging experiment, these data can be used to train a machine-learning (ML) model that maps the baseline GEO-FM carrier signal and observed frequency to an unknown level of encoder (Fig. 4C, detailed in Fig. S9). Using this approach, we experimentally calibrated GEO-FM circuit response across all possible carrier signals for the multi-component GEO we developed earlier, in which the slow *E. coli* Activator/ATPase provides the initial carrier signal, and the fast *P. damselae* activator acts as the encoder. The resulting ML model can decode any GEO-FM circuit's associated data and aids in development of specific circuit applications by providing a landscape of the FM response space to identify specific configurations with high dynamic range or high sensitivity.

Motivated by these results, we designed and implemented two GEO-FM circuits that encode single-cell dynamics operating at either gene-expression or post-translational timescales. To demonstrate a circuit that streams transcriptional activity, we placed the GEO-FM encoder under a doxycycline-inducible TetON promoter (Fig. 4E)[32]. In parallel, we designed a protein-level circuit that streams fast-timescale degradation activity by connecting the GEO-FM encoder to the drug-controllable DHFR degron (Fig. 4F)[33]. Here, the encoder is constitutively targeted for proteasomal destruction but can be rapidly stabilized upon addition of the small molecule TMP.

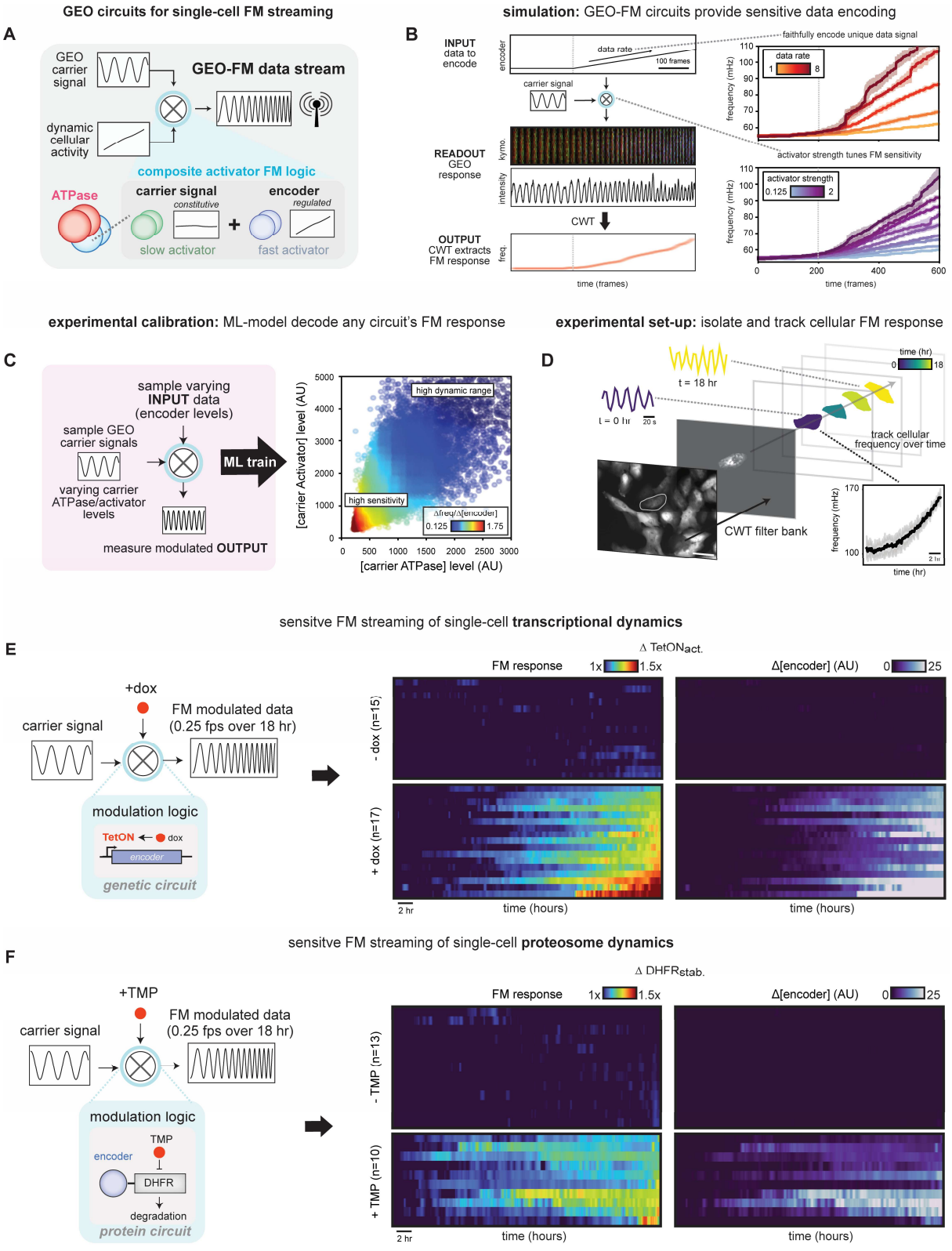

Figure 4. Design of FM data streaming circuits through dynamic regulation of multi-component composition. (A) Oscillating GEO signals act like a "cellular radio" that emits a unique genetically encoded frequency-barcoded signal. Circuits that stream single-cell data were designed by generating a carrier signal using an ATPase and slow carrier activator, then coupling the presence of a fast encoder activator to dynamic cellular activity. Cellular activity dynamics are encoded as resulting changes to frequency of the carrier signal. (B) The "skeleton model" from Fig. 3B was used to simulate GEO-FM circuit design. A simulated carrier waveform,

To quantify GEO-FM responses from these different circuits, cells were imaged at 0.25 fps for 18 hours using low intensity widefield fluorescence microscopy. Individual cells in complex cell culture mixtures were spectrally separated and tracked using CWT to follow single-cell frequency over time (Fig. 4D, detailed in Fig. S10, Movie S3).

For both circuits, single-cell GEO frequencies were stable in the absence of their small molecule inducer, showing little to no change over an 18-hour period. In contrast, the addition of inducer generated potent GEO-FM responses. Importantly, each GEO-FM circuit design produced a sensitive single-cell data stream that recapitulated the expected timescales of the dynamics at play[34]. For the transcriptional circuit, changes in GEO-FM signal took several hours to become detectable following doxycycline addition, after which they increased robustly over the course of the experiment. In contrast, GEO-FM signals for the degradation circuit were detected within less than an hour and rapidly reached a new steady state, owing to fast stabilization of the encoder.

Importantly, the FM responses for both circuit designs across any carrier signal could be decoded back into the underlying data of interest using the calibrated ML model we developed above. As such, our circuits can convert existing intensity-based reporter schemes into barcoded single-cell FM data streams measured in non-arbitrary units (ΔmHz) insensitive to photobleaching, fluorophore maturation times, and illumination intensity. Altogether, GEO-FM circuits are modular, sensitive, and readily designed tools that unlock noise-resistant FM data-encoding paradigms and open new avenues for dynamic single-cell imaging and analysis.

Discussion.

The GEO framework fulfills the demand for a high-performance biochemical analogue to the carrier signals that power modern telecommunications, unlocking a new paradigm for communicating live-cell biological information using frequency-modulated (FM) data transmission strategies. GEO-FM circuits that broadcast transcription and proteasome dynamics demonstrate robust multiplexed streaming of cell-state data, with high-sensitivity and high temporal resolution, while mitigating photobleaching and phototoxicity that traditionally hinder long microscopy experiments.

By harnessing the evolutionary diversity of MinDE-family ATPase/activator pairs[35], we expand the ability to program and manipulate these GEOs in human cells. We show that ATPase and activator components can be treated as separate modules, allowing for a small collection of functional components to be rationally combined, layered into composites, or dynamically controlled to build a large application space for GEO circuits. The extensive characterization and modeling of GEO circuits we performed defines parameters that reflect biochemical features of the GEO components, enabling straightforward design of GEO waveform behavior at scale.

---

composed of an ATPase and a carrier activator, was provided data in the form of a ramped increase of an encoder activator into the system. The simulated waveform was tracked to measure GEO response, and CWT was used to extract FM response. Simulations with altered input data rates and altered encoder activator strengths are shown. (C) A machine-learning model was trained using aggregated data from thousands of U-2 OS cells with a broad range of ATPase, carrier activator, and encoder activator levels, and the corresponding oscillation frequency of the circuit configuration. FM response sensitivity across ATPase and carrier activator expression levels is shown. (D) Example behavior of a GEO-FM circuit in a U-2 OS cell. A widefield fluorescence microscopy image of a representative cell in a complex cell culture mixture is shown (scale bar: 50μM). This cell is isolated in the frequency domain using CWT for downstream quantification and tracking. Visualization of segmentation tracks for this cell across the 18-hour time course is shown. Segmentation cell masks are color-coded by time to visualize movement of the cell body during the time course. Pixel-level time series for the cell is shown for 0-hr and 18-hr time points. Single-cell frequency is extracted from continuous waveform signal at 0.25 fps resolution for 18 hours. (E) Schematic of GEO-FM circuit design to encode transcription factor or (F) proteasomal degradation dynamics. To encode transcription factor activity, a genetic circuit placing an encoder activator under the control of the doxycycline-induced TetON promoter was designed. To encode proteasomal degradation dynamics, a protein circuit placing an encoder activator under the control of a TMP-stabilized DHFR degron was designed. Single-cell activity trajectories extracted using the frequency-barcoded FM response broadcast by the cells is shown, ordered by weakest to strongest final FM response. The FM response was converted to encoder expression level changes using the ML-model.

Our approach of engineering synthetic circuits to manipulate the spatiotemporal dynamics of a fluorescent protein in a cell is a strategy that complements efforts that engineer new biophysical properties into fluorescent proteins (FPs) directly. FP engineering typically targets the chemical environment of a chromophore to create new colors with altered excitation/emission or introduce photo-switching or photo-conversion activity[36–38]. However, spectral overlaps between optimized FP combinations fundamentally limits the number of usable channels[39,40]. FLIM methods or FPs with distinct photo-switching times can exploit the timescale of an exponentially decaying fluorescent signal to further increase the number of usable channels[41–44], but presently have palettes limited by our ability to understand and engineer the electronic state transitions at play.

In contrast, GEO approaches use synthetic biochemical circuitry[45–50] to integrate a cell's biology into the dynamics of an FP, thus coupling cellular identity and internal state to the stream of emitted photons over time. This creates a wide range of distinct single-cell imaging channels separable by frequency (6-205 mHz), rather than color, for multiplexing and data-encoding applications with whatever FPs are most appropriate for the biological system at hand. While FPs with different fluorescence properties are essential and necessary for imaging cellular structures or ultrafast signaling processes, GEOs complement these tools by providing a dynamic tunable medium for communicating single-cell data over most biologically relevant timescales.

This ability to use a cell's GEO frequency to encode dynamic single-cell information provides new capabilities and advantages over traditional fluorescent cell-state measurement. First, FM-encoded data is represented in the frequency domain, thus robust against intensity fluctuations and photobleaching, eliminating background and providing a high level of noise-rejection. Second, frequency, unlike intensity, is non-arbitrary. Single-cell data collected using different magnifications, fluorophores, or imaging setups can be directly compared or aggregated. Third, cells can stream their data on different frequency channels using the same fluorescent proteins, allowing unambiguous assignment and tracking of signals even from physically overlapping cells. Further evolutionary exploration within the MinDE/ParAB superfamily could potentially identify orthogonal ATPase/Activator pairs that allow multiple GEOs to operate in the same cell or use different surfaces, such as nucleic acids, to support their oscillation[24,26]. Together, these advantages allow GEOs to serve as a powerful high-performance data-encoding medium whose temporal structure facilitates acquisition and analysis of single-cell dynamics in real time.

Acknowledgements.

We thank members of the Coyle Lab, A. Weeks, W. Bement, W. Lim, and K. Roybal for advice, helpful discussions, and critical reading of the manuscript.

Funding: This work was supported by a David and Lucille Packard Fellowship for Science and Engineering (SMC) and NIH New Innovator award 1DP2GM154329-01 (SMC). RR was supported in part by the National Institute of General Medical Sciences of the National Institutes of Health under Award Number T32GM008505 (Chemistry–Biology Interface Training Program). DB was supported in part by a Biotechnology Training Program NIH 5 T32 TGM135066A.

Author contributions: RR and SMC conceived the overall project. The experimental plan was implemented by RR, TG, ZX, DB, EZWW and SMC. RR collected all experimental data for the paper with assistance from TG; except for that in Fig. 4E-F, which were performed by TG, and Fig. S4, which were performed by DB and EZWW. ZX performed the bioinformatic and evolutionary analysis in Fig. 1B and S1D. RR and SMC prepared the figures and wrote the manuscript with suggestions from all authors. SMC supervised all aspects of the work.

Competing interests: A provisional patent application has been filed by the University of Wisconsin and the Wisconsin Alumni Research Foundation related to this work.

References.

1. Purvis, J.E., and Lahav, G. (2013). Encoding and Decoding Cellular Information through Signaling Dynamics. *Cell 152*, 945–956.
2. Pollard, T.D., and Borisy, G.G. (2003). Cellular Motility Driven by Assembly and Disassembly of Actin Filaments. *Cell 112*, 453–465.
3. Gasch, A.P., Spellman, P.T., Kao, C.M., Carmel-Harel, O., Eisen, M.B., Storz, G., Botstein, D., and Brown, P.O. (2000). Genomic Expression Programs in the Response of Yeast Cells to Environmental Changes. *Mol. Biol. Cell 11*, 4241–4257.
4. Bar-Joseph, Z., Gitter, A., and Simon, I. (2012). Studying and modelling dynamic biological processes using time-series gene expression data. *Nat. Rev. Genet. 13*, 552–564.
5. Kalisky, T., and Quake, S.R. (2011). Single-cell genomics. *Nat. Methods 8*, 311–314.
6. Regev, A., Teichmann, S.A., Lander, E.S., Amit, I., Benoist, C., Birney, E., Bodenmiller, B., Campbell, P., Carninci, P., Clatworthy, M., et al. (2017). The Human Cell Atlas. *Elife 6*, e27041.
7. Kelly, R.T. (2020). Single-cell Proteomics: Progress and Prospects. *Mol. Cell. Proteom. 19*, 1739–1748.
8. Cusanovich, D.A., Daza, R., Adey, A., Pliner, H.A., Christiansen, L., Gunderson, K.L., Steemers, F.J., Trapnell, C., and Shendure, J. (2015). Multiplex single-cell profiling of chromatin accessibility by combinatorial cellular indexing. *Science 348*, 910–914.
9. Spiller, D.G., Wood, C.D., Rand, D.A., and White, M.R.H. (2010). Measurement of single-cell dynamics. *Nature 465*, 736–745.
10. Young, J.W., Locke, J.C.W., Altinok, A., Rosenfeld, N., Bacarian, T., Swain, P.S., Mjolsness, E., and Elowitz, M.B. (2012). Measuring single-cell gene expression dynamics in bacteria using fluorescence time-lapse microscopy. *Nat. Protoc*. *7*, 80–88.
11. Kudo, T., Jeknić, S., Macklin, D.N., Akhter, S., Hughey, J.J., Regot, S., and Covert, M.W. (2018). Live-cell measurements of kinase activity in single cells using translocation reporters. *Nat Protoc 13*, 155–169.
12. Regot, S., Hughey, J.J., Bajar, B.T., Carrasco, S., and Covert, M.W. (2014). High-Sensitivity Measurements of Multiple Kinase Activities in Live Single Cells. *Cell 157*, 1724–1734.
13. Ni, Q., Titov, D.V., and Zhang, J. (2006). Analyzing protein kinase dynamics in living cells with FRET reporters. *Methods 40*, 279–286.
14. Allen, M.D., and Zhang, J. (2006). Subcellular dynamics of protein kinase A activity visualized by FRET-based reporters. *Biochem Bioph Res Co 348*, 716–721.
15. Zhang, Q., Huang, H., Zhang, L., Wu, R., Chung, C.-I., Zhang, S.-Q., Torra, J., Schepis, A., Coughlin, S.R., Kornberg, T.B., et al. (2018). Visualizing Dynamics of Cell Signaling In Vivo with a Phase Separation-Based Kinase Reporter. *Mol. Cell 69*, 334-346.e4.
16. Linghu, C., Johnson, S.L., Valdes, P.A., Shemesh, O.A., Park, W.M., Park, D., Piatkevich, K.D., Wassie, A.T., Liu, Y., An, B., et al. (2020). Spatial Multiplexing of Fluorescent Reporters for Imaging Signaling Network Dynamics. *Cell 183*, 1682-1698.e24.
17. Skylaki, S., Hilsenbeck, O., and Schroeder, T. (2016). Challenges in long-term imaging and quantification of single-cell dynamics. *Nat. Biotechnol. 34*, 1137–1144.
18. Armstrong, E.H. (1936). A Method of Reducing Disturbances in Radio Signaling by a System of Frequency Modulation. *Proc. Inst. Radio Eng. 24*, 689–740.
19. Sturley, K.R. (1945). Frequency modulation. *J. Inst. Electr. Eng*. - Part III: Radio Commun. Eng. *92*, 197–213.
20. Banelli, P., Buzzi, S., Colavolpe, G., Modenini, A., Rusek, F., and Ugolini, A. (2014). Modulation Formats and Waveforms for 5G Networks: Who Will Be the Heir of OFDM?: An overview of alternative modulation schemes for improved spectral efficiency. *IEEE Signal Process. Mag. 31*, 80–93.
21. Rajasekaran, R., Chang, C.-C., Weix, E.W.Z., Galateo, T.M., and Coyle, S.M. (2024). A programmable reaction-diffusion system for spatiotemporal cell signaling circuit design. *Cell 187*, 345-359.e16.
22. Loose, M., Kruse, K., and Schwille, P. (2011). Protein Self-Organization: Lessons from the Min System. *Annu. Rev. Biophys. 40*, 315–336.
23. Vecchiarelli, A.G., Li, M., Mizuuchi, M., Hwang, L.C., Seol, Y., Neuman, K.C., and Mizuuchi, K. (2016). Membrane-bound MinDE complex acts as a toggle switch that drives Min oscillation coupled to cytoplasmic depletion of MinD. *Proc National Acad Sci 113*, E1479–E1488.
24. Lutkenhaus, J. (2012). The ParA/MinD family puts things in their place. *Trends Microbiol 20*, 411–418.
25. Ramm, B., Heermann, T., and Schwille, P. (2019). The E. coli MinCDE system in the regulation of protein patterns and gradients. *Cell Mol Life Sci 76*, 4245–4273.
26. Pulianmackal, L.T., Limcaoco, J.M.I., Ravi, K., Yang, S., Zhang, J., Tran, M.K., O'Meara, M.J., and Vecchiarelli, A.G. (2022). Multiple ParA/MinD ATPases coordinate the positioning of disparate cargos in a bacterial cell. *Biorxiv*, 2022.06.09.495121.

27. Fange, D., and Elf, J. (2006). Noise-Induced Min Phenotypes in E. coli. *PLoS Comput. Biol. 2*, e80.
28. Tomita, M., Hashimoto, K., Takahashi, K., Shimizu, T.S., Matsuzaki, Y., Miyoshi, F., Saito, K., Tanida, S., Yugi, K., Venter, J.C., et al. (1999). E-CELL: software environment for whole-cell simulation. *Bioinformatics 15*, 72–84.
29. Bjorklund, G.C., Levenson, M.D., Lenth, W., and Ortiz, C. (1983). Frequency modulation (FM) spectroscopy. *Appl. Phys.* B *32*, 145–152.
30. McDonnell, J.T.E., and Bentley, P.M. (1994). Wavelet transforms: an introduction. *Electron Commun Eng 6*, 175–186.
31. Sinha, S., Routh, P.S., Anno, P.D., and Castagna, J.P. (2005). Spectral decomposition of seismic data with continuous-wavelet transform. *Geophysics 70*, P19–P25.
32. Das, A.T., Tenenbaum, L., and Berkhout, B. (2016). Tet-On Systems For Doxycycline-inducible Gene Expression. *Curr. Gene Ther. 16*, 156–167.
33. Iwamoto, M., Björklund, T., Lundberg, C., Kirik, D., and Wandless, T.J. (2010). A General Chemical Method to Regulate Protein Stability in the Mammalian Central Nervous System. *Chem. Biol. 17*, 981–988.
34. Shamir, M., Bar-On, Y., Phillips, R., and Milo, R. (2016). SnapShot: Timescales in Cell Biology. *Cell 164*, 1302-1302.e1.
35. Pulianmackal, L.T., Limcaoco, J.M.I., Ravi, K., Yang, S., Zhang, J., Tran, M.K., Ghalmi, M., O'Meara, M.J., and Vecchiarelli, A.G. (2023). Multiple ParA/MinD ATPases coordinate the positioning of disparate cargos in a bacterial cell. *Nat. Commun. 14*, 3255.
36. Tsien, R.Y. (1998). The green fluorescent protein. *Biochemistry 67*, 509–544.
37. Shaner, N.C., Patterson, G.H., and Davidson, M.W. (2007). Advances in fluorescent protein technology. *J. Cell Sci. 120*, 4247–4260.
38. Adam, V., Berardozzi, R., Byrdin, M., and Bourgeois, D. (2014). Phototransformable fluorescent proteins: Future challenges. *Curr. Opin. Chem. Biol. 20*, 92–102.
39. Day, R.N., and Davidson, M.W. (2009). The fluorescent protein palette: tools for cellular imaging. *Chem. Soc. Rev. 38*, 2887–2921.
40. Higuchi-Sanabria, R., Garcia, E.J., Tomoiaga, D., Munteanu, E.L., Feinstein, P., and Pon, L.A. (2016). Characterization of Fluorescent Proteins for Three- and Four-Color Live-Cell Imaging in S. cerevisiae. *PLoS ONE 11*, e0146120.
41. Datta, R., Heaster, T.M., Sharick, J.T., Gillette, A.A., and Skala, M.C. (2020). Fluorescence lifetime imaging microscopy: fundamentals and advances in instrumentation, analysis, and applications. *J. Biomed. Opt. 25*, 071203–071203.
42. Becker, W. (2012). Fluorescence lifetime imaging – techniques and applications. *J. Microsc. 247*, 119–136.
43. Qian, Y., Celiker, O.T., Wang, Z., Guner-Ataman, B., and Boyden, E.S. (2023). Temporally multiplexed imaging of dynamic signaling networks in living cells. *Cell 186*, 5656-5672.e21.
44. Zhou, X.X., and Lin, M.Z. (2013). Photoswitchable fluorescent proteins: ten years of colorful chemistry and exciting applications. *Curr. Opin. Chem. Biol. 17*, 682–690.
45. Mukherji, S., and Oudenaarden, A. van (2009). Synthetic biology: understanding biological design from synthetic circuits. *Nat. Rev. Genet. 10*, 859–871.
46. Nandagopal, N., and Elowitz, M.B. (2011). Synthetic Biology: Integrated Gene Circuits. *Science 333*, 1244–1248.
47. Khalil, A.S., Lu, T.K., Bashor, C.J., Ramirez, C.L., Pyenson, N.C., Joung, J.K., and Collins, J.J. (2012). A Synthetic Biology Framework for Programming Eukaryotic Transcription Functions. *Cell 150*, 647–658.
48. Elowitz, M.B., and Leibler, S. (2000). A synthetic oscillatory network of transcriptional regulators. *Nature 403*, 335–338.
49. Chen, Z., and Elowitz, M.B. (2021). Programmable protein circuit design. *Cell 184*, 2284–2301.
50. Chen, Z. (2023). Protein circuit design using de novo proteins. *Trends Biotechnol. 41*, 593–594.